

Changes in Aggregation Patterns Detected by Diffusion, Viscosity, and Surface Tension in Water + 2-(Diethylamino)Ethanol Mixtures at Different Temperatures

Isabel M. S. Lampreia, Ângela F. S. Santos,* Maria João A. Barbas, Fernando J. V. Santos, and Manuel L. S. Matos Lopes

Departamento de Química e Bioquímica, Centro de Ciências Moleculares e Materiais, Faculdade de Ciências, Universidade de Lisboa, ed. C8 Campo Grande, 1749-016 Lisboa, Portugal

Mutual diffusion coefficients for 2-(diethylamino)ethanol (2) in water (1) were experimentally obtained by the Taylor dispersion technique from $x_2 = 0$ to ≈ 0.2 , at $T = 298$ K and $T = 303$ K. Viscosities and surface tensions were measured in the entire composition range using capillary viscometry and ring tensiometry, respectively. Viscosities were measured at the above temperatures, and surface tensions were measured at intervals of 5 K in the temperature range from (283 to 303) K. Information about intermolecular interactions, hydration modes, and solute aggregation is provided through the combined study of the observed changes in diffusion coefficients, viscosities, and surface tension with composition. Conclusions obtained are compared with those taken from volumetric and optical properties for the same system.

Introduction

Thermophysical properties of aqueous mixtures of aminoalcohols have received considerable attention in the recent literature^{1–9} in view of their application in removal of acidic gases, such as carbon dioxide and principally hydrogen sulfide, from process gas streams in the petroleum and natural gas industries.

In connection with that important application, the knowledge of different equilibrium and transport properties and their variation with composition and temperature is useful to extend our understanding of molecular interactions in solution, which in conjunction with molecular models is essential to either predict other properties or improve the design of gas-treating processes.

On the basis of density, ultrasound speed, and refractive index measurements reported in previous studies,^{10–12} we obtained apparent and excess partial molar properties for the binary mixture water + 2-(diethylamino)ethanol (DEEA). In this work, we present experimental data on mutual diffusion coefficients, dynamic viscosities, and surface tension. Diffusion studies in aqueous systems were found to be a sensitive measure of changes in the water structure induced by solutes.¹³ Effects of association can also be inferred from the observed changes in mobility of the dissolved species.^{14,15} In this work, the combination of measured diffusion coefficients with dynamic viscosity data allowed us to derive correlation lengths, giving additional information regarding intermolecular interactions operating in the water-rich region. On the other hand, viscosity data combined with densities lead to the evaluation of the volume of solvent bound per unit mass of solute giving information about volume changes connected with the hydration process as a function of temperature. Finally, the concentration dependence of the surface tension of the aqueous DEEA solutions was analyzed at several temperatures. On the basis of these data, the relative Gibbs adsorption isotherm was used to evaluate the critical aggregation concentration as well as the energetic and

surface-packing efficiency. Exploring further correlations between surface and bulk properties of these aqueous solutions, composition dependences of surface entropy, S^S , and enthalpy, H^S , have also been obtained.

Experimental Section

Chemicals. 2-(Diethylamino)ethanol, CAS number 100-37-8, was a reagent-grade product supplied by Merck (99 % quoted purity) and was used without further purification. Its purity was tested by density measurement, $d = 879.50$ kg·m⁻³ at $T = 298.15$ K and $d = 884.14$ kg·m⁻³ at $T = 293.15$ K. Literature values reported for the same temperatures² are $d = 879.54$ kg·m⁻³ and $d = 884.20$ kg·m⁻³, respectively.

High purity water of grade 1 (ISO3696:1995(E)) from a Milli-Q system supplied by Millipore was used to prepare all solutions.

Measurements. Mixtures were prepared by mass using a Mettler AX 205 balance measuring within ± 0.01 mg. Buoyancy corrections were applied. Care has been taken in the solutions preparation to prevent evaporation. Special vessels were used as previously described.¹⁶

Kinematic viscosities, ν , at atmospheric pressure were measured using 6 Ostwald type glass capillary viscometers (sizes A, B, and C) made by Cannon and 3 Ubbelohde type glass capillary viscometers made by Schott—Geräte (sizes 0c, 0a, and I). Flow times were measured by a photoelectric detector (ViscoClock made by Schott) using infrared light gates with a resolution of 0.01 s and a reproducibility of ± 0.04 %. The temperature has been set to within ± 0.003 K using a Tamson thermostat (TMV 40) and measured with an uncertainty of ± 0.02 K, with a semistandard Pt100, using a multimeter (Keithley 196). Both thermometer and multimeter have been calibrated in the ITS-90 scale.

The Ostwald viscometers were calibrated at the experimental temperatures by a step-up procedure based on water satisfying ISO3696:1995(E) requisites for grade 1, using kinematic viscosity values from ISO/TR3666:1998(E), while the Ubbelohde viscometers belonged to an NP EN ISO/IEC 17025 accredited calibration laboratory and were calibrated using both a step-up

* Corresponding author. E-mail: afsantos@fc.ul.pt. Fax: +351217500088. Tel: +351217500915.

procedure and Cannon viscosity standards. Viscometers of sizes A and 0c were directly calibrated with water at two different temperatures, while other sizes were calibrated with 2 oils whose viscosities were more than 50 % apart. The viscosity of each of those oils was established by measurements with both viscometers of the previous size. Calibrations were further verified using a set of oil-based calibration standards supplied by Cannon Instrument Co. so as to exclude the presence of surface tension effects in the step-up procedure. Dynamic viscosities were calculated using the working equation

$$\eta/\rho = kt \quad (1)$$

where ρ and η are the density and dynamic viscosity, respectively, t is the flow time, and k is the viscometer constant. As a supplemental test for the presence of surface tension effects, the experimental values measured for 298.15 K were obtained using all nine different viscometers of both Ostwald and Ubbelohde types. The Ostwald type viscometers are generally preferred to avoid surface tension effects, but measurements made with Ubbelohde viscometers showed agreement within experimental uncertainty, indicating the absence of surface tension effects. No signal of calibration artifacts was detected on the viscosity curves. The viscosity values for 303.15 K were obtained using just the six Ostwald viscometers. For each composition, the most suitable viscometer was chosen to avoid the need for the introduction of Hagenbach corrections. This selection was based on the evaluation of the Hagenbach constant for each viscometer to establish the minimum flow time ensuring an uncertainty in measured flow time higher than the Hagenbach correction. The estimated uncertainty for viscosity data depends on the essay with the median being 0.33 % ($k = 2$) and the average being 0.45 % ($k = 2$), not taking into account the uncertainty on the viscosity of water. Densities were calculated from experimental values reported in refs 10 and 11 by least-squares fitting of the data to fifth degree polynomial equations.

Mutual diffusion coefficients, D_{12} , were measured by the Taylor dispersion method using an apparatus that has already been described elsewhere.¹⁷ Some improvements have been introduced, namely the replacement of the previous detector by a new differential refractometer (Waters, model 2410). To ensure that the instrument operated in accordance with the supporting theory, experiments were carried out at various flow speeds. Results demonstrated optimal experimental conditions for flow rates conducting to diffusion times of about 15 ks. Mole fraction differences between injected solutions ($x_2 + \Delta x_2$) and carrier solutions (x_2) were in the order of 0.007 or less. To ensure that the measured diffusion coefficients were independent of the initial concentration difference, solutions of different compositions were injected into each carrier. Reported D_{12} values were determined from 3 to 5 replicate dispersion profiles. The median of the reproducibility of the method for the whole set of mean D_{12} values was found to be ± 1 % and the uncertainty of the mutual diffusion coefficients is estimated to be in the order of 2 %.

Surface tensions, γ , were measured by the ring method, with an interfacial tensiometer, Krüss K8, equipped with a 20 mm diameter platinum–iridium ring. A F6 Haake thermostat has been used to circulate water through the tensiometer thermostat vessel to maintain the temperature constant to within ± 0.1 K. The temperature was measured with a mercury in glass thermometer with an uncertainty of ± 0.3 K, calibrated against a standard platinum resistance thermometer (SPRT), calibrated by the National Physical Laboratory in the International Temperature Scale ITS-90. Each surface tension value reported

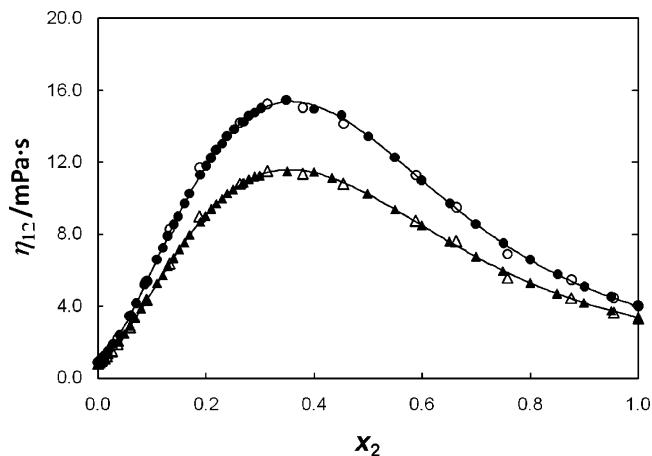


Figure 1. Composition dependence of the viscosity for the water (1) + 2-(diethylamino)ethanol (2) system at two temperatures: ●, this work at $T = 298.15$ K; ▲, this work at $T = 303.15$ K; ○, ref 6 at $T = 298.15$ K; △, ref 6 at $T = 303.15$ K. Full lines represent polynomial fitting equations.

Table 1. Experimental Viscosity Values η_{12} for the Binary System Water (1) + 2-(diethylamino)ethanol (2) at $T = (298.15$ and $303.15)$ K

x_2	$T/K = 298.15$		$T/K = 303.15$				
	η_{12} mPa·s	η_{12} mPa·s	η_{12} mPa·s	η_{12} mPa·s			
0.00000	0.890	0.24008	13.418	0.00000	0.794	0.24980	10.478
0.01005	1.201	0.25302	13.843	0.01005	1.062	0.26736	10.836
0.02016	1.536	0.26736	14.240	0.02016	1.333	0.27008	10.859
0.03000	1.949	0.27008	14.252	0.03976	2.025	0.28008	11.046
0.04005	2.421	0.28008	14.548	0.05015	2.464	0.29002	11.207
0.05946	3.473	0.29002	14.764	0.06028	2.899	0.30033	11.246
0.06152	3.510	0.30219	14.985	0.07004	3.354	0.35001	11.498
0.07026	4.128	0.34998	15.430	0.08051	3.860	0.39965	11.471
0.08762	5.181	0.39992	14.977	0.08982	4.289	0.43299	11.121
0.09008	5.347	0.45066	14.581	0.11005	5.269	0.49950	10.243
0.11005	6.615	0.50007	13.447	0.12003	5.728	0.54983	9.382
0.12003	7.243	0.55038	12.285	0.13008	6.216	0.59971	8.485
0.13008	7.863	0.60012	10.959	0.14007	6.673	0.64986	7.581
0.14007	8.511	0.65141	9.672	0.15113	7.151	0.70009	6.746
0.14830	8.960	0.70005	8.576	0.16025	7.537	0.74978	5.970
0.16025	9.677	0.75077	7.471	0.17038	7.965	0.79999	5.299
0.17038	10.258	0.80013	6.597	0.18969	8.687	0.84995	4.701
0.19047	11.306	0.85076	5.743	0.19985	9.003	0.90003	4.196
0.20040	11.763	0.90009	5.063	0.21042	9.393	0.94999	3.742
0.21042	12.222	0.95009	4.494	0.22000	9.709	1.00000	3.375
0.22000	12.662	1.00000	4.010	0.23006	9.979		
0.23006	13.043			0.24008	10.256		

was an average of 4 to 8 measurements, and the repeatability was found to be ± 0.02 mN·m⁻¹. The accuracy of the measured surface tension values for pure water was found to be 0.5 mN·m⁻¹ and 0.03 mN·m⁻¹, at the lower and higher temperatures, respectively. The uncertainties were found to vary from 1.4 % at $T = 283.15$ K to 0.1 % at $T = 303.15$ K.

Results and Discussion

Viscosities. Dynamic viscosities for the aqueous solutions of 2-(diethylamino)ethanol at $T = (298.15$ and $303.15)$ K are reported in Table 1 and are shown in Figure 1 as a function of DEEA mole fraction, x_2 . Results obtained by Mather and co-workers⁶ are also shown in this figure. Clearly both sets of results match fairly well.

Viscosity deviations from the additive rule, representing the weighted mean viscosity of the pure components, were calculated using the following expression:

$$\Delta\eta = \eta_{12} - (x_1\eta_1^* + x_2\eta_2^*) \quad (2)$$

Table 2. Least-Squares A_k Coefficients of Eq 3 for the System Water + 2-(Diethylamino)ethanol at $T = 298.15$ K and $T = 303.15$ K^a

$A_k/\text{mPa}\cdot\text{s}$	$T = 298.15$ K	$T = 303.15$ K
A_0	44.057	32.530
A_1	-51.572	-36.904
A_2	6.675	7.168
A_3	37.778	21.461
A_4	-34.677	-25.520
A_5	9.343	11.513
$\sigma_{\text{fit}}/\text{mPa}\cdot\text{s}$	0.04	0.02

^a Standard deviations of the fits, σ_{fit} , are also given.

where η_{12} is the viscosity of the binary mixture, x_1 and x_2 are the mole fractions of water and DEEA, and η_1^* and η_2^* are the viscosities of pure water and pure DEEA, respectively. The number of experimental points and their internal consistency led us to choose a Redlich–Kister (R-K) equation of the form

$$\Delta\eta/\text{mPa}\cdot\text{s} = x_1x_2 \sum_{k=0}^{k=n} A_k(1 - 2x_2)^k \quad (3)$$

to correlate $\Delta\eta$ data. The number n of the A_k coefficients in this equation was fixed by testing the statistical significance of including each further term using the F test at a 95 % confidence level. The optimized number of these coefficients was found to be six (i.e., $n = 5$) for each isotherm. The values for these regression coefficients and the respective standard deviations are given in Table 2, together with the standard deviations of the fits. The strong positive deviations of viscosities comply well with the reported¹⁰ large negative excess molar volumes with extreme values located around the same composition (ca. $x_2 = 0.35$).

The fact that the momentum transport mechanism connected with the viscous flow depends on the extensive participation of surrounding solvent¹⁸ led some authors to relate specific volumes of hydrated solutes, calculated from experimental viscosity data on one hand and density data on the other.^{19,20} The procedure was first applied by Linow and Philipp¹⁹ to solutes such as glycol and glycerine and some electrolytes to get information on the hydration of the solute. Resorting to the mentioned procedure, we have then used our viscosity data to calculate specific volumes of the hydrated solute, $v_{\eta,2}$, by using eq 4. As our experimental values are sparse in the water very-rich region, we have also used the results obtained by Mather and co-workers⁶ at the two lowest concentrations ($x_{\text{DEEA}} = 0.0039$ and 0.0080).

$$v_{\eta,2} = \frac{\eta_{\text{sp}}}{c} \left(\frac{1}{f + \eta_{\text{sp}}} \right) \quad (4)$$

In eq 4, $\eta_{\text{sp}} = (\eta_{12} - \eta_1^*)/\eta_1^*$ is the specific viscosity of the solute, and c is its amount concentration expressed in gram of solute per cm^3 of solution. $f = 2.5$ is the numerical factor of the viscosity–concentration relation developed by Einstein and expressed by eq 5 as

$$\eta_r = \frac{\eta_{12}}{\eta_1^*} = 1 + 2.5\phi \quad (5)$$

In this equation, η_{12} , η_1^* , and η_r are the solution, pure solvent, and relative viscosities, respectively, and ϕ is the volume fraction of the particle in solution. As it is known, this equation

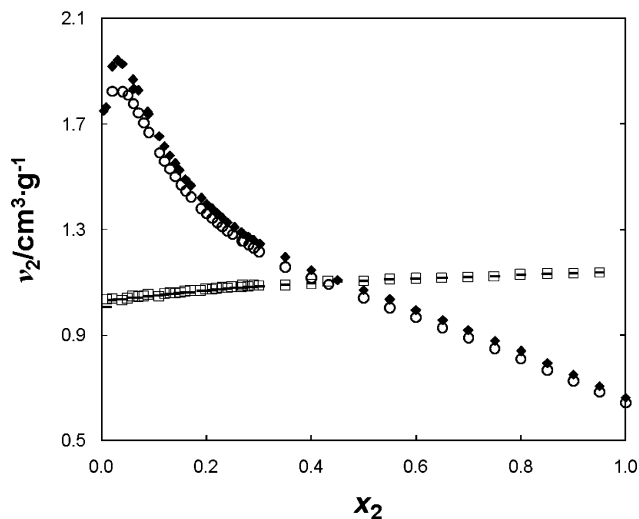


Figure 2. Specific volumes based on viscosity values, $v_{\eta,2}$, at \blacklozenge , $T = 298.15$ K; \circ , $T = 303.15$ K. Specific volumes based on density values, $v_{\phi,2}$, at \square , $T = 298.15$ K; \square , $T = 303.15$ K.

is valid when the dispersed particles are unsolvated, uniform-sized hard spheres.

On the other hand we have calculated the apparent specific volumes of DEEA, $v_{\phi,2}$, using eq 6 and density data previously reported^{10,11}

$$v_{\phi,2} = \frac{\rho_1^* - \rho}{m\rho\rho_1^*M_2} + \frac{1}{\rho} \quad (6)$$

In eq 6, m is the molality of the solute, M_2 is its molar mass, and ρ and ρ_1^* are densities of the solution and of the pure solvent, respectively. $v_{\eta,2}$ and $v_{\phi,2}$ values at $T = (298.15$ and $303.15)$ K are plotted in Figure 2. As can be seen in this figure, specific volumes based on viscosity values are much more sensitive to hydration features, with $v_{\eta,2} - v_{\phi,2}$ being a measure of the volume of solvent bound per gram of solute. Maximum values in $v_{\eta,2}$ are noticeable in the water-rich region suggesting important changes in the hydration scheme along this water-rich region.

The combination of eqs 4 and 6 has been used to calculate $(v_{\eta,2} - v_{\phi,2})$, which is related to the viscosity solute–solvent interaction strength parameter, called Magazù parameter,²⁰ \mathcal{M}

$$\mathcal{M} = \frac{\rho(v_{\eta,2} - v_{\phi,2})M_2}{M_1} \quad (7)$$

where M_1 is the molar mass of the solvent. Plots of \mathcal{M} as a function of amount concentration, c , at the two experimental temperatures are displayed in Figure 3. Extrapolation to infinite dilution of the parameter \mathcal{M} gives the hydration number, n_h^η , this being the number of moles of solute-bonded water molecules present in the inner hydration sphere, per mole of solute.

In this way, we obtained $n_h^\eta = 4.0$ and 3.5 at $T = (298.15$ and $303.15)$ K, respectively. This result is consistent with predominant solute–solvent H-bond interactions acting in this water very-rich region, which indeed is expected to decrease when temperature increases.

Mutual Diffusion Coefficients. Diffusion results for the examined binary system, obtained in the mole fraction range from $x_2 = 0$ to $x_2 = 0.2$, are reported in Table 4 at $T = (298.15$ and $303.15)$ K and are plotted in Figure 4. The mutual diffusion

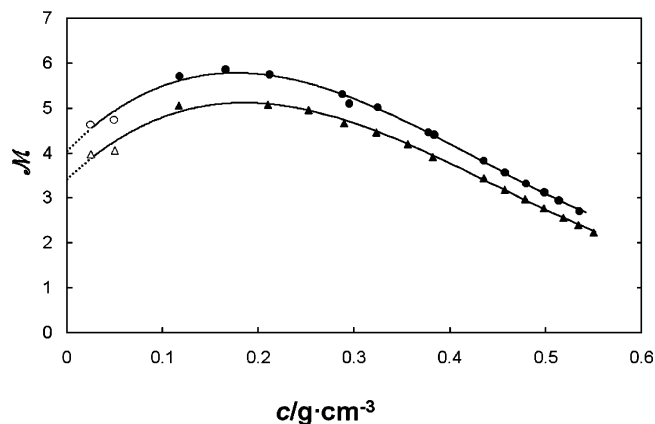


Figure 3. Magazú parameter, M , as a function of concentration, $c/\text{g}\cdot\text{cm}^{-3}$, at two temperatures: ●, this work at $T = 298.15$ K; ○, calculated with viscosity data from ref 6 at $T = 298.15$ K; ▲, this work at $T = 303.15$ K; △, calculated with viscosity data from ref 6 at $T = 303.15$ K. Full lines represent polynomial fitting equations and dotted lines are extrapolations of M to infinite dilution.

Table 3. Fitted Values for the b_i Parameters of Eq 8 at $T = 298.15$ K and $T = 303.15$ K^a

T K	$10^{10} b_0$ $\text{m}^2\cdot\text{s}^{-1}$	$10^{10} b_1$ $\text{m}^2\cdot\text{s}^{-1}$	$10^{10} b_2$ $\text{m}^2\cdot\text{s}^{-1}$	$10^{10} b_3$ $\text{m}^2\cdot\text{s}^{-1}$	$10^{10} b_4$ $\text{m}^2\cdot\text{s}^{-1}$	$10^{10} \sigma_{\text{fit}}$ $\text{m}^2\cdot\text{s}^{-1}$
298.15	6.83	-157.52	1665.39	-7722.78	12707.60	0.06
303.15	7.53	-177.35	2012.75	-10467.50	20531.87	0.1

^a Standard deviations of the fits, σ_{fit} , are also given.

Table 4. Experimental Mutual Diffusion Coefficients D_{12} for the Binary System Water (1) + 2-(diethylamino)ethanol (2) at $T = 298.15$ K and $T = 303.15$ K

$10^{10} D_{12}/\text{m}^2\cdot\text{s}^{-1}$			
x_2	$T/\text{K} = 298.15$	x_2	$T/\text{K} = 303.15$
0.00427	6.17	0.00278	7.11
0.01425	4.95	0.00524	6.50
0.03523	2.95	0.00781	6.39
0.05087	2.23	0.01032	5.82
0.05118	2.22	0.01281	5.63
0.07013	1.58	0.01536	5.39
0.09711	1.32	0.01779	4.82
0.10044	1.26	0.02026	4.54
0.14671	1.07	0.02731	4.06
		0.03820	3.14
		0.05024	2.55
		0.07362	1.77
		0.09846	1.53
		0.12470	1.37
		0.14757	1.29
		0.18011	1.32

coefficients, D_{12} , were least-squares fitted to polynomial equations of the form

$$D_{12}/\text{m}^2\cdot\text{s}^{-1} = \sum_{i=0}^{i=n} b_i x_2^i \quad (8)$$

Best values for the regression coefficients, σ_{fit} , are given in Table 3 together with the standard deviations of the fits.

To gain a deeper insight into the origin of significant changes in mobility of the dissolved species, highlighted by the decrease of D_{12} at low concentrations, we compared the observed behavior of the diffusion coefficient with that found near a consolute or pseudo-consolute point, where the size of the aggregates formed can be represented by a correlation length, ξ .¹³ Using the classical relation of Stokes–Einstein for the

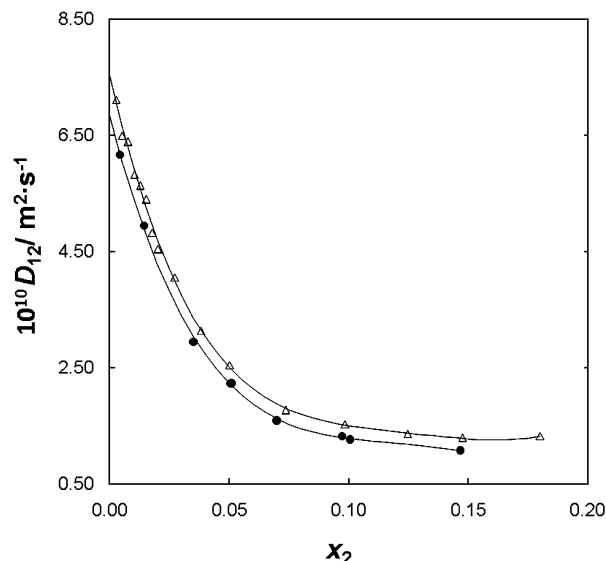


Figure 4. Mutual diffusion coefficients for water (1) + 2-(diethylamino)ethanol (2) at ●, $T = 298.15$ K; △, $T = 303.15$ K. Full lines represent polynomial fitting equations.

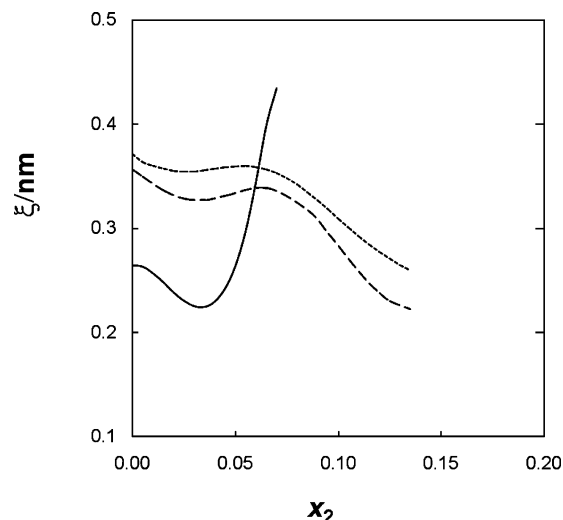


Figure 5. Correlation lengths, ξ , for water (1) + 2-(diethylamino)ethanol (2) mixtures at - · -, $T = 298.15$ K; - - -, $T = 303.15$ K; and for water (1) + t-butanol (2) - - -, at $T = 298.15$ K, calculated from data in ref 13.

Brownian motion of a particle of radius ξ , the mutual diffusion coefficient can be approached by eq 9 as

$$\xi = \frac{kT}{6\pi D_{12} \eta_{12}} \quad (9)$$

where k is the Boltzmann constant. Using this equation we have calculated the correlation length at $T = (298.15$ and $303.15)$ K for the aqueous solutions of DEEA. The results are shown in Figure 5 together with values for water + (2-methyl-propan-2-ol (TBA)).¹³ The latter system is referred to in the literature as a mixture where aggregates would be formed.^{21,22} The lack of a pronounced increase in the correlation length in water + DEEA curves, such as that observed in TBA, does not suggest the formation of hydrophobic–interaction driven aggregates. Nevertheless, in the x_2 available range the s-shaped curves displayed in Figure 5 may correspond to the existence of transition points related to mixing–scheme changes. Interestingly, the maximum observed around DEEA mole fraction of 0.07, shown in Figure 5, closely matches the sudden change in V_2^E , observed around $x_2 = 0.08$ in Figure 5 of ref 10. A similar

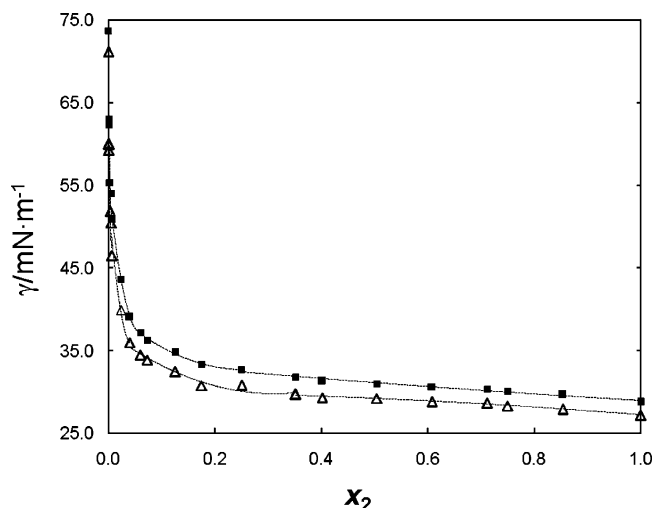


Figure 6. Surface tension, γ , versus liquid composition for the water (1) + 2-(diethylamino)ethanol (2) system at \blacksquare , $T = 283.15$ K; \triangle , $T = 303.15$ K. Lines are drawn as guides for the eye.

Table 5. Experimental Surface Tension Values γ for the Binary System Water (1) + 2-(diethylamino)ethanol (2) from $T = (283.15$ to $303.15)$ K

x_2	$\gamma/\text{mN}\cdot\text{m}^{-1}$				
	283.15 K	288.15 K	293.15 K	298.15 K	303.15 K
0.00000	73.74	73.14	72.59	71.84	71.20
0.00104	62.91	62.06	61.43	60.80	60.06
0.00111	62.83	61.98	61.34	60.70	59.95
0.00130	62.32	61.47	60.62	59.88	59.24
0.00336	55.32	54.27	53.43	52.59	51.86
0.00503	54.03	53.11	52.35	51.41	50.47
0.00679	50.98	49.93	48.58	47.43	46.50
0.02372	43.65	42.61	41.89	40.85	39.92
0.03998	39.05	38.43	37.60	36.88	35.96
0.06011	37.17	36.56	36.00	35.23	34.47
0.07276	36.26	35.84	35.06	34.59	33.87
0.12527	34.78	34.38	33.88	33.18	32.48
0.17488	33.38	32.58	32.18	31.58	30.78
0.25031	32.74	32.22	31.82	31.21	30.81
0.35154	31.85	31.24	30.73	30.22	29.72
0.40180	31.32	30.72	30.23	29.73	29.34
0.50381	31.02	30.62	30.22	29.72	29.22
0.60800	30.63	30.23	29.73	29.23	28.83
0.71205	30.36	29.96	29.66	29.15	28.65
0.75029	30.08	29.69	29.29	28.80	28.30
0.85420	29.69	29.30	28.80	28.41	27.91
1.00000	28.79	28.39	27.99	27.60	27.20

feature is also apparent in Figure 2 of ref 12, where the partial molar refraction of mixing of DEEA, $\Delta_{\text{mix}}R_2$, shows a minimum about this same composition. These singular features, which are now confirmed by independent equilibrium and transport properties, will probably correspond to changes in aggregation patterns.

Surface Tension. Experimental surface tensions, γ , were measured at five temperatures from $T = (283.15$ to $303.15)$ K at $T = 5$ K intervals. The values are reported in Table 5. The composition variation of the surface tension at two of the experimental temperatures is shown in Figure 6, where dashed curves are drawn as guides for the eye. Although in a milder way, when compared to a typical surfactant, surface tension at low DEEA concentrations shows a striking dependence on composition. The rapid decrease in surface tension indicates that this solute accumulates preferentially at the air/water interface. Furthermore, the tendency to a flattening out of the curves with increasing solute concentration indicates the presence of some kind of aggregates, pointing out further evidence of the aggregation tendency displayed by DEEA in aqueous

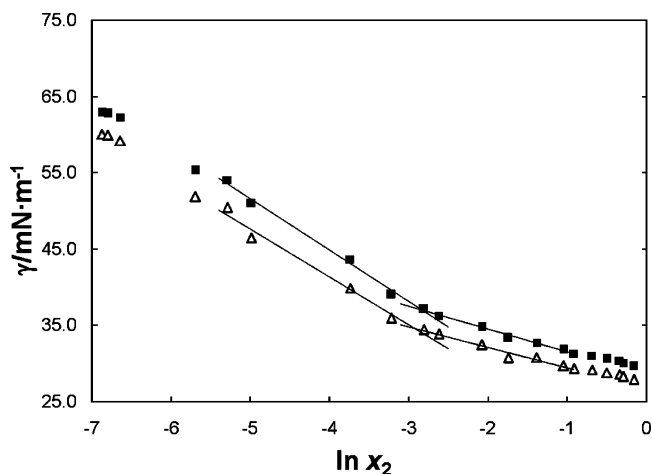


Figure 7. Gibbs adsorption isotherms for aqueous solutions of 2-(diethylamino)ethanol at \blacksquare , $T = 283.15$ K; \triangle , $T = 303.15$ K.

environment. To the end of a further clarification of this subject, a quantitative analysis of the experimental data, based on derived thermodynamic properties was made. To depict any particular feature, we have plotted in Figure 7 experimental γ values as a function of $\ln x_{\text{DEEA}}$ for the isotherms at $T = (283.15$ and $303.15)$ K as examples. In this figure, we can observe a noticeable change in the slope of the straight lines that least-squares fit the points, just before and after the break points shown. The corresponding concentrations were assumed to be the onset of the critical aggregation concentration (CAC). CAC values were then calculated from the interception of the straight lines for all the experimental temperatures and are shown in Table 6. Considering the associated uncertainties (standard deviations calculated with the usual propagation error analysis), the close matching of the tabulated CAC values with the aforementioned feature in the V_2^E curve about $x_2 = 0.08$ is again quite significant. Other aggregation parameters, namely aggregation Gibbs energy, ΔG_{CAC} , aggregation entropy, ΔS_{CAC} , and aggregation enthalpy, ΔH_{CAC} , were calculated, resorting to the usual pseudo-phase model, using eqs 10–12.

$$\Delta G_{\text{CAC}} = RT \ln x_{\text{CAC}} \quad (10)$$

$$\Delta S_{\text{CAC}} = -\left(\frac{\partial(\Delta G_{\text{CAC}})}{\partial T}\right)_P \quad (11)$$

$$\Delta H_{\text{CAC}} = \Delta G_{\text{CAC}} + T\Delta S_{\text{CAC}} \quad (12)$$

Thermodynamic properties of liquid/air interface such as the solute relative surface excess, $\Gamma_2^{(1)}$, and the surface areas per molecule, a_m , corresponding to saturated monolayers at the interface, were calculated using eq 13, which represents the relative Gibbs isotherm,²³ and eq 14, respectively.

$$\Gamma_2^{(1)} = -\frac{1}{RT} \left(\frac{\partial \gamma}{\partial \ln a_2} \right)_T \quad (13)$$

$$a_m = \frac{1}{N_A \Gamma_2^{(1)}} \quad (14)$$

In dilute solutions, the solute activity coefficient, a_2 , can be regarded as unity, and therefore in eq 13 the mole fraction can be used instead of activity. $\Gamma_2^{(1)}$ values at the five experimental temperatures were thus calculated using the slopes of the lines fitted below the breaking points of the plots, γ versus $\ln x_{\text{DEEA}}$. In eq 14, N_A is the Avogadro's constant. All the above-mentioned calculated values are presented in Table 6. The

Table 6. Aggregation Parameters and Thermodynamic Properties of the Liquid/Air Interface in the System Water + DEEA

T K	$CAC(x_{DEEA})$	ΔG_{CAC} kJ·mol ⁻¹	ΔS_{CAC} J·mol ⁻¹ ·K ⁻¹	ΔH_{CAC} kJ·mol ⁻¹	$10^6\Gamma_2^{(1)}$ mol·m ⁻²	a_m nm ²
283.15	0.060 ± 0.02	-6.62 ± 0.03			2.86 ± 0.1	0.581 ± 0.02
288.15	0.057 ± 0.02	-6.86 ± 0.03			2.75 ± 0.1	0.605 ± 0.03
293.15	0.056 ± 0.03	-7.03 ± 0.04	35.9 ± 1.6	3.5 ± 0.5	2.63 ± 0.2	0.631 ± 0.04
298.15	0.055 ± 0.04	-7.19 ± 0.04			2.54 ± 0.2	0.654 ± 0.05
303.15	0.054 ± 0.04	-7.36 ± 0.04			2.48 ± 0.2	0.670 ± 0.05

decreasing or increasing trend with increasing temperature displayed by some of the values shown in Table 6, such as CAC, $\Gamma_2^{(1)}$, and a_m , are all in agreement with the general temperature dependence exhibited by other nonionic amphiphiles in water.^{24–26}

Negative ΔG_{CAC} values would mean that DEEA spontaneously forms some kind of aggregates in aqueous solution, and positive ΔS_{CAC} and ΔH_{CAC} values are an indication that the aggregation process is entropically driven as already stated by other authors.^{25,26}

The temperature dependence of γ at fixed compositions was used to further estimate surface entropy^{23,27}

$$S^s = -\left(\frac{\partial\gamma}{\partial T}\right)_{x,P} \quad (15)$$

as well as surface enthalpy

$$H^s = \gamma - T\left(\frac{\partial\gamma}{\partial T}\right)_{x,P} \quad (16)$$

For any given concentration of DEEA and in the temperature range studied, the surface tension of the mixture was found to decrease linearly with increasing temperature. Surface entropy values were then obtained from the slopes of the γ versus T linear plots at DEEA fixed compositions and are plotted in Figure 8. The pattern found is identical with that displayed for alcohol + water mixtures²⁸ and isobutylamine + water mixtures,²⁹ where one or two maxima were observed in the water-rich region. Despite the several competing processes ascribed by the authors to explain this behavior, namely hydrophobic hydration, formation of aggregates of solute molecules at the interface, dimer formation, and others, relevance was given to the fact that rapid structural changes occur at very low solute concentrations. This seems to comply with our previous supposition that important conformation changes in DEEA molecules would take place at the water very-rich region,¹⁰ namely, that there would be a displacement of the equilibrium

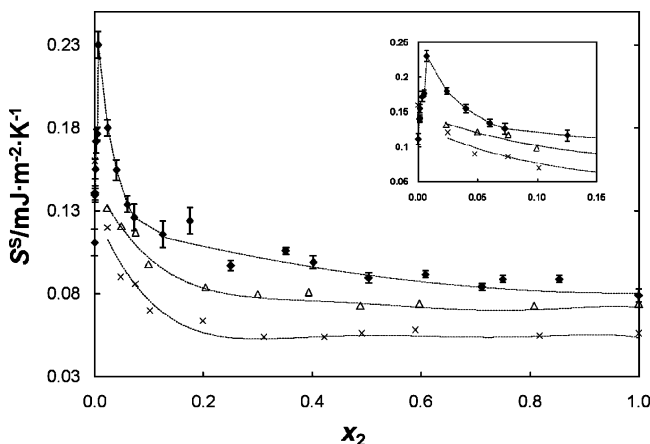


Figure 8. The entropy of surface formation plotted versus the concentration of solute: \blacklozenge , DEEA this work in the temperature range $T = (283.15$ to $303.15)$ K; Δ , DMEA; \times , MDEA ref 30 in the temperature range $T = (298.15$ to $328.15)$ K. Lines are drawn as guides for the eye.

Table 7. Surface Thermodynamics of Pure DEEA,^a DMEA,^b and MDEA^b

	$\gamma/\text{mN}\cdot\text{m}^{-1}$ (at $T = 298.15$ K)	$S^s/\text{mJ}\cdot\text{m}^{-2}\cdot\text{K}^{-1}$ (in exp. temp. ranges)	$H^s/\text{mJ}\cdot\text{m}^{-2}$ (at $T = 298.15$ K)
DEEA ^a	27.6	0.08	51
DMEA ^b	31.5	0.07	54
MDEA ^b	38.3	0.06	55

^a Present work. ^b Ref 30.

between rotamers toward the predominance of gauche interactions. The present results are also in line with those obtained by Maham and Mather³⁰ for aqueous solutions of alkylethanolamines with hydrophobic hydrocarbon tails very similar to that of DEEA. As can be seen in Figure 8, where the results obtained by these authors are also shown the variation of surface entropy for our system is analogous to those found for water + methyl diethanolamine (MDEA), and water + dimethyl ethanolamine (DMEA). Moreover S^s values for the same composition are in the order MDEA < DMEA < DEEA, which supports the explanation already enunciated by Mather et al.³¹ that the number and length of end alkyl groups have important effects on the surface properties of these aqueous solutions. The absence of maxima for water + MDEA and water + DMEA mixtures is possibly due to the fact that they are located at composition values lower than the lowest mole fraction obtained by the referred to authors. Further evidence of the effect of the hydrophobic tails can be observed in Table 7 where values of the surface properties of pure MDEA, DMEA, and DEEA are presented.

Finally, it should be mentioned that surface enthalpy values obtained for water/DEEA mixtures are positive and follow the pattern found for surface entropy. A sharp maximum at $x_{DEEA} \approx 0.003$ is followed by an effective stabilization.

Conclusions

By combining viscosity and density data obtained in the water very-rich region, in this work we were able to calculate hydration numbers, $n_h^H = 4.0$ and 3.5 at $T = (298.15$ and $303.15)$ K, respectively, for water + DEEA mixtures. This decrease observed with increasing temperature is in accordance with the solute–solvent H-bond interactions in the very dilute region.

Additionally, by relating mutual diffusion coefficients and viscosity data in the composition range $x_{DEEA} = 0$ to $x_{DEEA} = 0.2$, we have calculated correlation lengths that led us to confirm transition points apparently related to changes in mixing aggregation pattern by independent methods.

Furthermore, surface tension measurements strongly suggest that phenomena in the bulk is reflected on the surface and allowed us to obtain quantitative values for the critical aggregation concentration, CAC, as a function of temperature. Additional analysis based on surface entropy and enthalpy values, when compared with those already published in similar amphiphilic systems, emphasizes the importance of the role played by the number and length of end alkyl groups on surface properties.

Acknowledgment

The authors thank Professor J. C. Reis for the revision of the manuscript.

Literature Cited

- (1) Li, J.; Mundhwa, M.; Tontiwachwuthikul, P.; Henni, A. Volumetric Properties, Viscosities, and Refractive Indices for Aqueous 2-(Methylamino)ethanol Solutions from (298.15 to 343.15) K. *J. Chem. Eng. Data* **2007**, *52*, 560–565.
- (2) Álvarez, E.; Gómez-Díaz, D.; La Rubia, M. D.; Navaza, J. M. Densities and Viscosities of Aqueous Ternary Mixtures of 2-(Methylamino)ethanol and 2-(Ethylamino)ethanol with Diethanolamine, Triethanolamine, *N*-Methyldiethanolamine, or 2-Amino-1-methyl-1-propanol from 298.15 K to 323.15 K. *J. Chem. Eng. Data* **2006**, *51*, 955–962.
- (3) Bernal-García, J. M.; Hall, K. R.; Estrada-Baltazar, A.; Iglesias-Silva, G. A. Density and Viscosity of Aqueous Solutions of *N,N*-Dimethylethanolamine at $p = 0.1$ MPa from $T = (293.15 \text{ to } 363.15)$ K. *J. Chem. Thermodyn.* **2005**, *37*, 762–767.
- (4) Álvarez, E.; Cancela, A.; Maceiras, R.; Navaza, J. M.; Táboas, R. Surface Tension of Aqueous Binary Mixtures of 1-Amino-2-Propanol and 3-Amino-1-Propanol, and Aqueous Ternary Mixtures of These Amines with Diethanolamine, Triethanolamine, and 2-Amino-2-methyl-1-propanol from (298.15 to 323.15) K. *J. Chem. Eng. Data* **2003**, *48*, 32–35.
- (5) Chan, C.; Maham, Y.; Mather, A. E.; Mathonat, C. Densities and Volumetric Properties of the Aqueous Solutions of 2-Amino-2-Methyl-1-Propanol, *n*-Butyldiethanolamine, and *n*-Propylethanolamine at Temperatures from 298.15 K to 353.15 K. *Fluid Phase Equilib.* **2002**, *198*, 239–250.
- (6) Maham, Y.; Lebrette, L.; Mather, A. E. Viscosities and Excess Properties of Aqueous Solutions of Mono- and Diethylethanolamines at Temperatures between 298.15 K and 353.15 K. *J. Chem. Eng. Data* **2002**, *47*, 550–553.
- (7) Hawrylak, B.; Burke, S. E.; Palepu, R. Partial Molar and Excess Volumes and Adiabatic Compressibilities of Binary Mixtures of Ethanolamines with Water. *J. Solution Chem.* **2000**, *29*, 575–594.
- (8) Zhang, F. Q.; Li, H. P.; Dai, M.; Zhao, J. P. Volumetric Properties of Binary Mixtures of Water with Ethanolamine Alkyl Derivatives. *Thermochim. Acta* **1995**, *254*, 347–357.
- (9) Hikita, H.; Ishikawa, H.; Uku, K.; Murakami, T. Diffusivities of Mono-, Di-, and Triethanolamines in Aqueous Solutions. *J. Chem. Eng. Data* **1980**, *25*, 324–325.
- (10) Barbas, M. J. A.; Dias, F. A.; Mendonça, A. F. S. S.; Lampreia, I. M. S. Volumetric Properties of Aqueous Binary Mixtures of 2-Diethylaminoethanol from 283.15 K to 303.15 K. *Phys. Chem. Chem. Phys.* **2000**, *2*, 4858–4863.
- (11) Lampreia, I. M. S.; Dias, F. A.; Mendonça, A. F. S. S. Isobaric Expansions and Isentropic Compressions of Aqueous Binary Mixtures of 2-Diethylaminoethanol from 283 K to 303 K. *Phys. Chem. Chem. Phys.* **2003**, *5*, 1419–1425.
- (12) Lampreia, I. M. S.; Mendonça, A. F. S. S.; Dias, S. M. A.; Reis, J. C. R. New Tools for the Analysis of Refractive Index Measurements in Liquid Mixtures. Application to 2-Diethylaminoethanol + Water mixtures from 283.15 K to 303.15 K. *New J. Chem.* **2006**, *30*, 609–614.
- (13) Harris, K. R.; Lam, H. N. Mutual-Diffusion Coefficients and Viscosities for the Water–2-Methylpropan-2-ol System at 15 °C and 25 °C. *J. Chem. Soc., Faraday Trans.* **1995**, *91*, 4071–4077.
- (14) Leaist, D. G. Diffusion in Associating Nonelectrolyte Mixtures: Stepwise Aggregation and Micelle Formation. *Can. J. Chem.* **1988**, *66*, 1129–1134.
- (15) Hao, L.; Lu, R.; Leaist, D. G.; Poulin, P. R. Aggregation Number of Aqueous Sodium Cholate Micelles from Mutual Diffusion Measurements. *J. Solution Chem.* **1997**, *26*, 113–125.
- (16) Barbosa, E. F. G.; Lampreia, I. M. S. Partial Molal Volumes of Amines in Benzene. Specific interactions. *Can. J. Chem.* **1986**, *64*, 387–393.
- (17) Matos Lopes, M. L.; Nieto de Castro, C. A.; Sengers, J. V. Mutual Diffusivity of a mixture of *n*-Hexane and Nitrobenzene Near Its Consolute Point. *Int. J. Thermophys.* **1992**, *13*, 283–293.
- (18) Stokes, R. H.; Mills, R. Viscosity of Electrolytes and Related Properties. In *International Encyclopedia of Physical Chemistry and Chemical Physics*, Topic 16; Pergamon Press: Oxford, 1965; Vol. 3.
- (19) Linow, K.-J.; Philipp, B. Die Konzentrationsabhängigkeit der Viskosität – ein neuer Weg zur Ermittlung von Solvatationszahlen. *Z. Phys. Chem.* **1984**, *265*, 321–329.
- (20) Branca, C.; Magazù, S.; Maisano, G.; Migliardo, F.; Migliardo, P.; Romeo, G. Hydration Study of PEG/Water by Quasi Elastic Light Scattering, Acoustic, and Rheological Measurements. *J. Phys. Chem. B* **2002**, *106*, 10272–10276.
- (21) Ito, N.; Kato, T.; Fujiyama, T. Determination of Local Structure and Moving Unit Formed in Binary Solution of *t*-Butyl Alcohol and Water. *Bull. Chem. Soc. Jpn.* **1981**, *54*, 2573–2578.
- (22) Nishikawa, K.; Iijima, T. Structural Study of *tert*-Butyl Alcohol and Water Mixtures by X-ray Diffraction. *J. Phys. Chem.* **1990**, *94*, 6227–6231.
- (23) Adamson, A. W. *Physical Chemistry of Surfaces*, 5th ed.; John Wiley and Sons: New York, 1990.
- (24) Holmberg, K.; Jonsson, B.; Kronberg, B.; Lindman, B. *Surfactants and Polymers in Aqueous Solution*; John Wiley and Sons: New York, 1999.
- (25) Rosen, M. J.; Cohen, A. W.; Dahanayake, M.; Hua, X.-Y. Relationship of Structure to Properties in Surfactants. 10. Surface and Thermodynamic Properties of 2-Dodecyloxy poly(ethoxyethanol)s, C₁₂H₂₅(OC₂H₄)_xOH, in Aqueous Solution. *J. Chem. Phys.* **1982**, *86*, 541–545.
- (26) Smith, S.; Wiseman, P.; Boudreau, L.; Marangoni, G.; Palepu, R. Effect of Microheterogeneity on Bulk and Surface Properties of Binary Mixtures of Polyoxyethylene Glycol Monobutyl Ethers with Water. *J. Solution Chem.* **1994**, *23*, 207–222.
- (27) Hansen, R. S. Thermodynamics of Interfaces Between Condensed Phases. *J. Phys. Chem.* **1962**, *66*, 410–415.
- (28) Gliniski, J.; Chavepeyer, G.; Platten, J.-K. Surface Properties of Diluted Aqueous Solutions of 1,2-Pentanediol. *J. Chem. Phys.* **1999**, *111*, 3233–3236.
- (29) Gliniski, J.; Chavepeyer, G.; Platten, J.-K. Surface Properties of Diluted Aqueous Solutions of Solutes Containing Isopropyl Hydrophobic Group. *J. Chem. Phys.* **2001**, *114*, 5702–5706.
- (30) Maham, Y.; Mather, A. E. Surface Thermodynamics of Aqueous Solutions of Alkylethanolamines. *Fluid Phase Equilib.* **2001**, *182*, 325–336.
- (31) Maham, Y.; Chevillard, A.; Mather, A. E. Surface Thermodynamics of Aqueous Solutions of Morpholine and Methylmorpholine. *J. Chem. Eng. Data* **2004**, *49*, 411–415.

Received for review June 22, 2007. Accepted August 15, 2007. The authors thank the Portuguese Foundation for Science and Technology FCT and FEDER for financial support to the research project POCTI/QUI/14265/2001.

JE700350B